

## Electronic Supplementary Information (ESI)

### Super-flexible bis(trifluoromethanesulfonyl)-amide doped graphene transparent conductive electrode for photo-stable perovskite solar cells

Jin Hyuck Heo, Dong Hee Shin, Do Hun Kim, Sang Jin Lee and Sang Hyuk Im\*

Department of Chemical and Biological Engineering, Korea University, 145 Anam-ro, Seongbuk-gu, Seoul 136-713, Republic of Korea

E-mail: imromy@korea.ac.kr

#### Experimental Section

##### 1. Preparation of TFSA doped graphene.

Monolayer graphene film was produced by 70- $\mu\text{m}$ -thick Cu-foils (Wacopa, 99.8 purity)-catalyzed chemical vapor deposition at 1000 °C for 30 min under flow of  $\text{CH}_4$  (30 sccm) and  $\text{H}_2$  (10 sccm) at a pressure of 10 Torr. After the growth of graphene film/Cu foil, a poly(methyl methacrylate) (PMMA) or PDMS solution was drop-coated onto the graphene sheet/Cu foil and then annealed at 180 °C for 1 min or 150 °C for 30 min, respectively. The Cu foil was etched away using an  $\text{FeCl}_3$  etchant (Sigma-Aldrich) for 2 h or 1 M ammonium persulfate solution for 10 h to obtain a PMMA-coated graphene or PDMS-coated graphene film, respectively. Sequentially, the PMMA layer was removed by immersing in an acetone bath for 1 hour to prepare a clean graphene sheet. TFSA powder (Sigma-Aldrich) used for p-type dopant was dissolved in nitromethane at concentrations ( $n_D$ ) of 10, 20, and 30 mM for preparing TFSA doping solution. For the doping of graphene, the dopant solution was dropped on the whole surface of graphene sheet and after 2 min elapsed, it was spin-coated at 2500 rpm for 1 min.

##### 2. Characterization of graphene electrodes.

The transmittance and sheet resistance, and work function of TFSA-doped graphene electrodes were measured by ultraviolet-visible-near IR optical spectrometer (Agilent Model) and the 4 probe van der Pauw method (Dasol eng, model FPP-HS8-40K), and Kevin probe force microscopy (Park systems, model XE100), respectively, and its surface morphology was analyzed by atomic force microscopy with non-contact mode (Park systems, model XE100). The atomic bonding states of the TFSA/graphene were characterized by X-ray XPS using Al  $\text{K}\alpha$  line of 1486.6 eV. The Raman spectra were measured by laser excitation energy of 532 nm (2.33 eV) with a power and spot size of 1mW and 1  $\mu\text{m}$ . Hall-effect measurements were performed by van der Pauw method (Ecopia model HEM-2000). The change in sheet resistance of the TFSA-doped graphene due to substrate bending can be expressed as  $\Delta R = (R - R_0)/R_0$ , where  $R_0$  is the initial measured resistance, and  $R$  is the resistance measured under substrate bending.

##### 3. Fabrication of perovskite solar cells.

PEDOT:PSS (Clevios P VP Al 4083) was spin-coated on an TFSA-doped graphene (or pristine graphene) surface/glass or PDMS at 3000 rpm for 60 s and then annealed at 150 °C for 20 min, respectively. For the  $\text{FAPbI}_{3-x}\text{Br}_x$  layer, we prepared  $\text{PbI}_2(\text{DMSO})_2$  complex by dissolving 50 g  $\text{PbI}_2$  in 150 mL dimethylsulfoxide (DMSO, Aldrich) at 60 °C for 30 min, and then 350

mL toluene slowly dropped into the  $\text{PbI}_2$  solution. The white precipitate was filtered and was annealed in vacuum oven at 60 °C for 5h to obtain  $\text{PbI}_2(\text{DMSO})$  complex. 1 M  $\text{PbI}_2(\text{DMSO})$  complex was dissolved in N,N-dimethylformamide (DMF, Aldrich) at 60 °C for 5 min. The  $\text{PbI}_2(\text{DMSO})$  complex solution was coated by spin coating at 3000 rpm for 30 s followed by spin-coating of 0.5 M FAI and MABr (0.85:0.15 mol:mol) mixture solution in iso-propanol (IPA, Aldrich) at 5000 rpm for 30 s. The film tuned from clear to dark brown during spin-coating was dried on the hot plate at 150 °C 20 min. After that, PCBM (nano-C) in toluene (20 mg per 1 mL) solution was coated onto the perovskite layer at 2000 rpm for 60 s. Finally, the device was transferred to a vacuum chamber for Al electrode evaporation. Whole experiments were conducted under controlled relative humidity of below 25 wt%. The active area was fixed to 0.16 cm<sup>2</sup>.

#### 4. Characterization of solar cells.

The photovoltaic properties of the cells were measured using a solar simulator (Pecell, PEC-L01) under illumination of 1 Sun (100 mWcm<sup>-2</sup> AM 1.5G) and a calibrated Si reference cell certificated by Japanese Industrial Standards. The external quantum efficiency (EQE) was measured by a power source (ABET 150 W xenon lamp, 13014) with a monochromator (DongWoo Optron, MonoRa-500i). The bending tests of cells were conducted using bars with radius of 2, 4, 6, 8, 10 and 12 mm, and continuous bending test jigs. All bending tests were conducted at 0.5 Hz bending frequency at room temperature. The stability tests were conducted using solar simulator without UV cut filter, which is ABA grade (spectral coincidence: class A/JIS C8912, uniformity: class B/JIS C8912 and temporal fluctuation: class A/JIS C8912) and air-conditioning chamber. The stability tests were conducted under 1 Sun illumination at 60 °C and 30 % relative humidity.

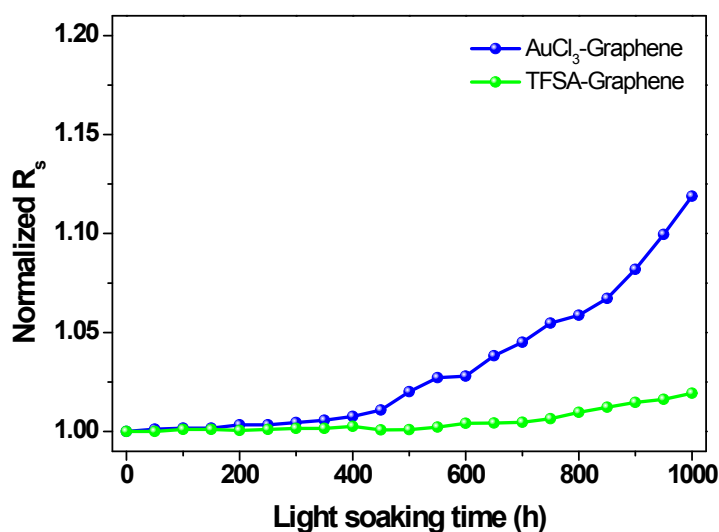


**Figure S1.** The sheet resistance ( $R_s$ ) of TFSA-doped and  $\text{AuCl}_3$ -doped GR TCE with continuous light soaking time for 1000 h.

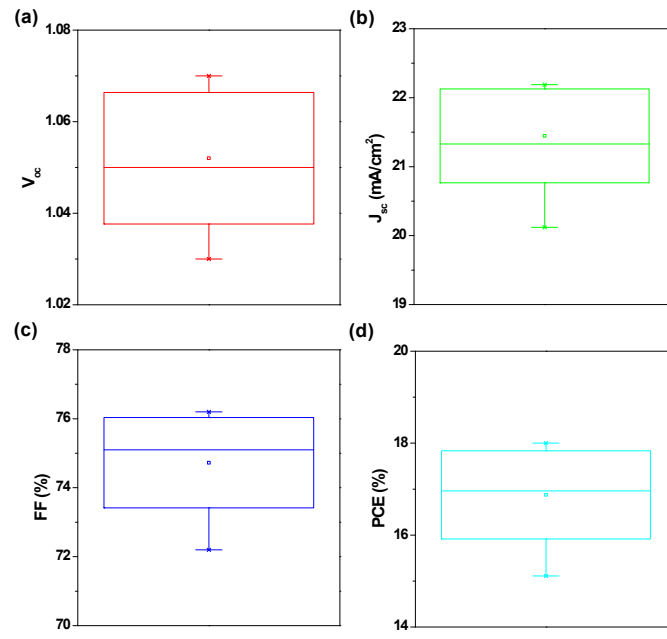
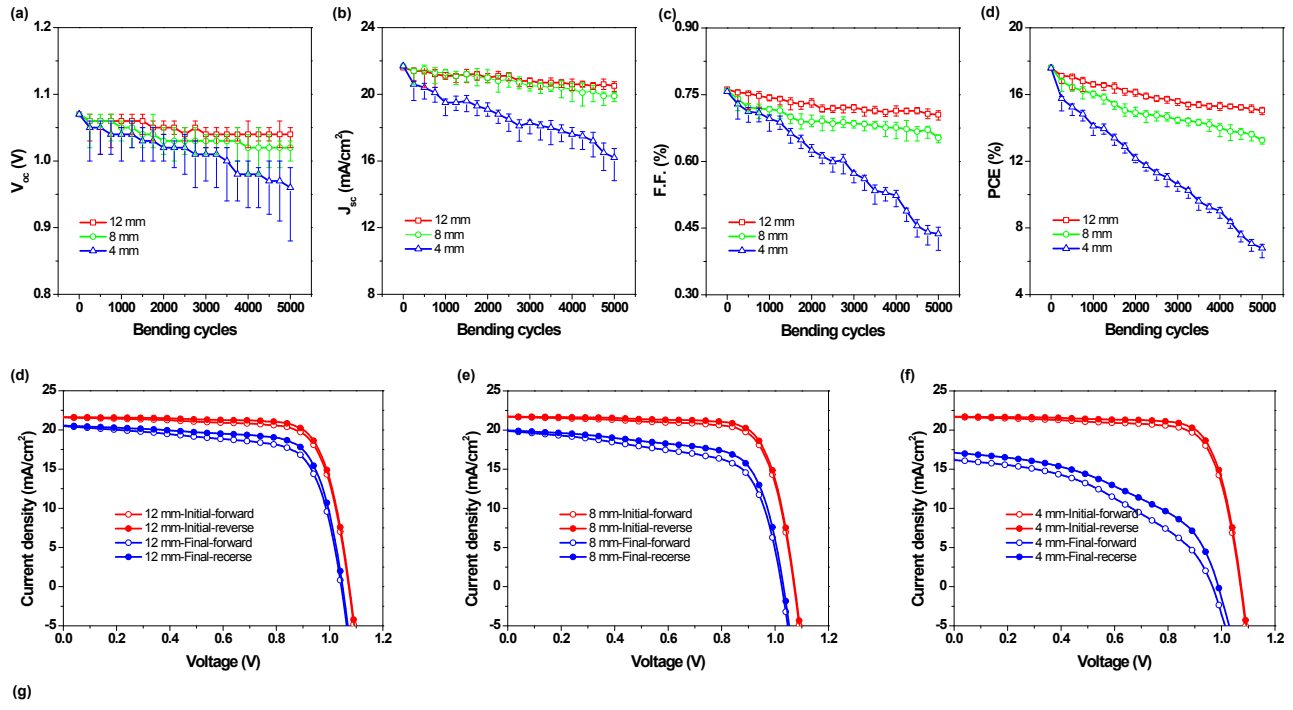
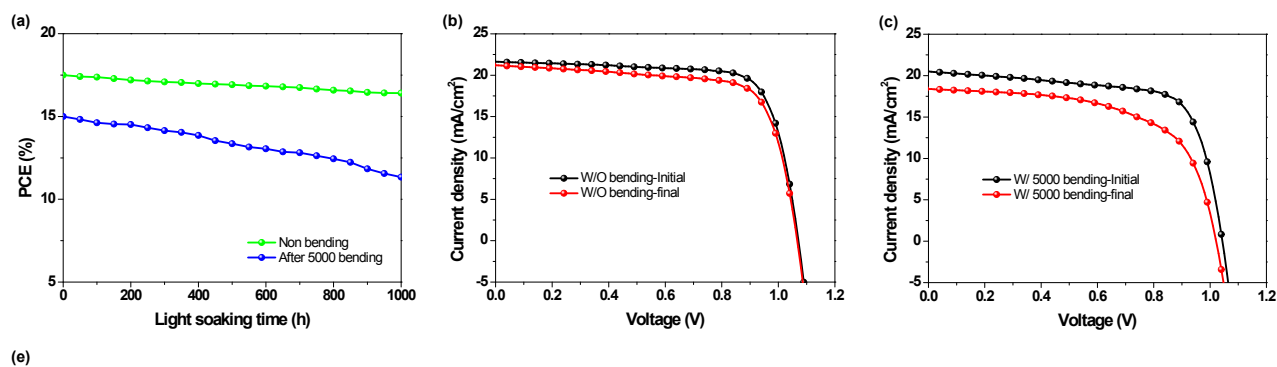


**Figure S2.** Box plots of 20 samples for average photovoltaic parameters of flexible device: (a)  $V_{oc}$ , (b)  $J_{sc}$ , (c) FF, (d) PCE



Device type	Scan direction	$V_{oc}$ (V)	$J_{sc}$ (mA/cm <sup>2</sup> )	F.F.(%)	$\eta$ (%)
12 mm-initial	Forward	1.07	21.6	76.2	17.6
	Reverse	1.07	21.6	78	18.0
12 mm-final	Forward	1.04	20.5	70.5	15.0
	Reverse	1.04	20.6	74.3	15.9
8 mm-initial	Forward	1.07	21.7	75.9	17.6
	Reverse	1.07	21.7	77.7	18.0
8 mm-final	Forward	1.02	19.9	65.3	13.3
	Reverse	1.03	20.0	69.3	14.3
4 mm-initial	Forward	1.07	21.7	75.7	17.6
	Reverse	1.07	21.7	77.9	18.1
4 mm-final	Forward	0.96	16.2	43.7	6.8
	Reverse	0.98	17.1	46.8	7.8

**Figure S3.** (a-d) the photovoltaic parameters of flexible devices at R = 12, 8, and 4 mm during 5000 bending tests, (d-e) their  $J-V$  curves of before and after bending test, and (g) summary of photovoltaic properties of flexible devices before and after bending test.



Device type	Condition	$V_{oc}(V)$	$J_{sc}(mA/cm^2)$	F.F(%)	$\eta(\%)$
W/O bending test	Initial	1.07	21.6	75.6	17.5
	Final	1.06	21.2	73.0	16.4
W/ bending test	Initial	1.04	20.5	70.5	15.0
	Final	1.02	18.4	60.4	11.3

**Figure S4.** (a) long-term stability test of flexible device with and without 5000 cycles bending test under 60 °C, 30 % relative humidity, and 1 sun illumination conditions for 1000 h. (b, c)  $J$ - $V$  curves of flexible device with and without 5000 cycles bending test at initial and final state, and (e) summary of photovoltaic properties of flexible device with and without 5000 cycles bending test.

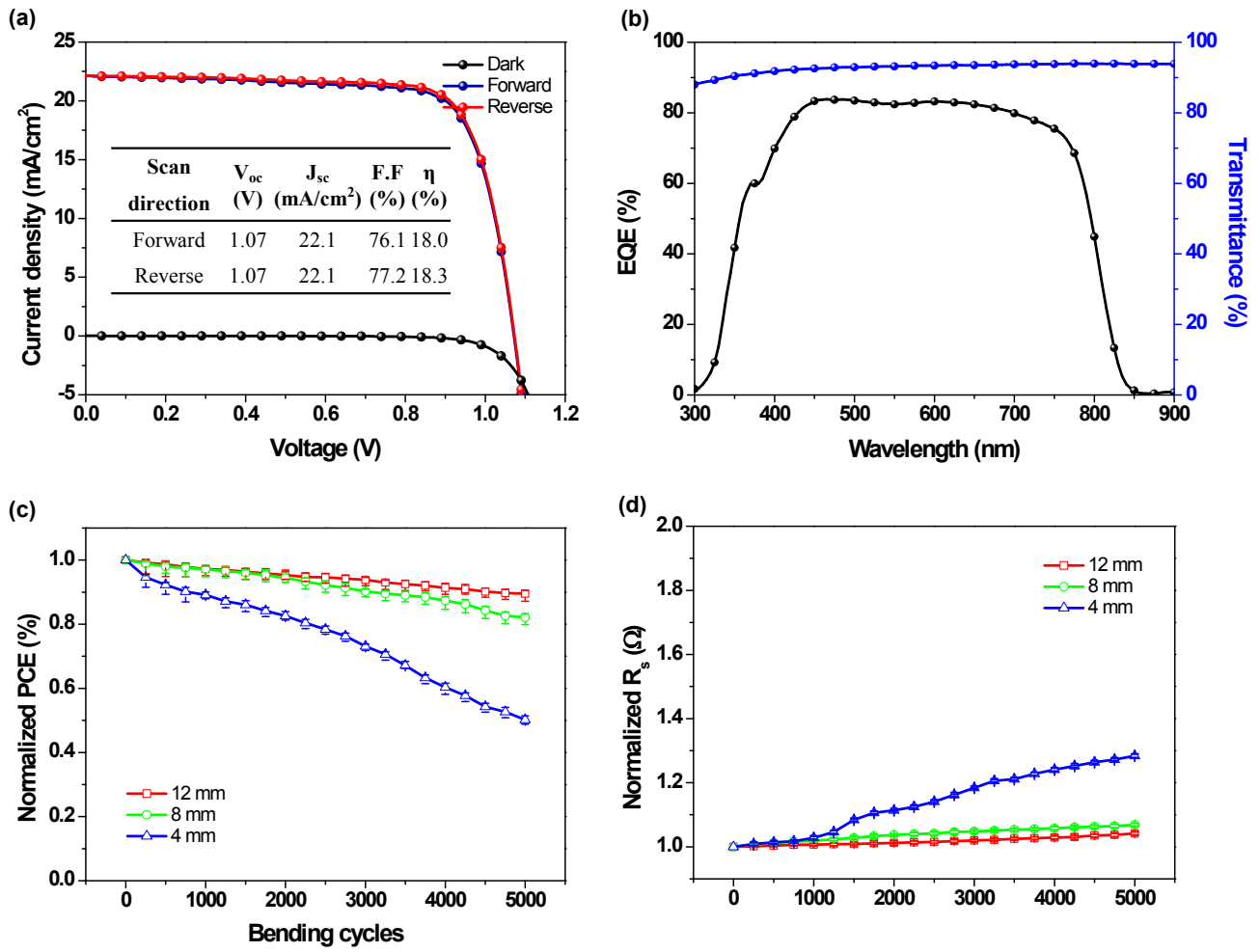


**Figure S5.** (a) J-V curves of APTES treated TFSI-doped Gr TCE based flexible perovskite solar cells, (b) Transmittance of APTES treated TFSI-doped Gr TCE and EQE spectrum of APTES treated TFSI-doped Gr TCE based flexible perovskite solar cells, (c) normalized PCEs of APTES treated TFSI-doped Gr TCE based flexible perovskite solar cells with bending cycles, and (d) normalized sheet resistance of APTES treated TFSI-doped Gr TCE with bending cycles.